Interactions of Thrombin with Fibrinogen Adsorbed on Methyl-, Hydroxyl-, Amine-, and Carboxyl-Terminated Self-Assembled Monolayers†

Kenyon M. Evans-Nguyen,‡ Lauren R. Tolles,‡ Oleg V. Gorkun,§ Susan T. Lord,*,‡,§ and Mark H. Schoenfisch*,‡

Department of Chemistry, University of North Carolina, Chapel Hill, North Carolina 27599, and Department of Pathology and Laboratory Medicine, University of North Carolina, Chapel Hill, North Carolina 27599

Received July 21, 2005; Revised Manuscript Received September 26, 2005

ABSTRACT: We have examined the initial phase of fibrin formation, thrombin-catalyzed fibrinopeptide cleavage, from adsorbed fibrinogen using surface plasmon resonance and liquid chromatography−mass spectrometry. Fibrinogen adsorption impaired thrombin−fibrinogen interactions compared to the interactions of thrombin with fibrinogen in solution. The properties of the underlying substrate significantly affected the extent and kinetics of fibrinopeptide cleavage, and the conversion of adsorbed fibrinogen to fibrin. Fibrinogen adsorbed on negatively charged surfaces (carboxyl-terminated self-assembled monolayers) released a smaller amount of fibrinopeptides, at a reduced rate relative to those of hydrophobic, hydrophilic, and positively charged surfaces (methyl-, hydroxyl-, and amine-terminated self-assembled monolayers, respectively). Additionally, the conversion of adsorbed fibrinogen to fibrin was comparatively inefficient at the negatively charged surface. These data correlated well with trends previously reported for fibrin proliferation as a function of surface properties. We conclude that thrombin interactions with adsorbed fibrinogen determine the extent of subsequent fibrin proliferation on surfaces.

Biomedical materials are used for several million blood-contacting devices yearly, including vascular grafts, stents, catheters, and blood bags (*1*). Currently available materials for such devices are plagued with problems caused by the inherent biological response to blood contact (*2*). Future developments in controlling biological responses to blood-contacting biomaterials will be based on advances in understanding the biology of inflammation, wound healing, and thrombosis on surfaces (*3*).

Thrombosis on surfaces is generally believed to be mediated by a layer of plasma proteins that rapidly adsorb at the blood−material interface, initiating platelet adhesion and fibrin formation (*1*). The adsorption of plasma proteins at the blood−biomaterial interface and the relationship of adsorbed proteins, particularly fibrinogen, to platelet adhesion and activation have been studied extensively (*1*, *4*−*8*); however, few studies have examined the formation of fibrin on surfaces (*9*, *10*). Fibrin polymer is the major structural component of the provisional matrix that temporarily encapsulates foreign materials during the immune response (*4*, *11*, *12*). Little is known about the formation of the provisional matrix at the interface between blood and implanted materials.

Fibrinogen plays a pivotal role in thrombosis on surfaces and is present at high concentrations in the adsorbed plasma protein layer. Fibrinogen is the precursor to fibrin polymer, and it binds platelets to biomaterial surfaces (*4*, *13*, *14*). Fibrinogen is a 340 kDa plasma protein made up of two copies of three polypeptide chains: Aα, Bβ, and γ. The N-termini of each of the two sets of intertwined chains meet at the center of the molecule, the E domain. Fibrinogen is symmetric about the center, and each of the two sets of chains extends outward from the E domain as coiled-coil arms to form the terminal globular D domains containing the C terminus of the Bβ and γ chains. The C terminus of each of the Aα chains extends out from the D domains, through extended unfolded regions, ending in globular domains (*14*, *15*).

Fibrin polymerization is initiated when the enzyme thrombin interacts with the center of fibrinogen to catalyze the specific cleavage of the first 16 residues of the Aα chain (fibrinopeptide A, FpA), yielding fibrin monomer (*16*). After FpA cleavage occurs, the fibrin monomers spontaneously associate in a half-staggered orientation, resulting in the formation of protofibrils. Coincident to protofibril formation, thrombin catalyzes the cleavage of the first 14 residues of the Bβ chain (fibrinopeptide B, FpB), subsequently polymerizing the protofibrils. The resulting weblike fibrin polymer binds platelets and other cells and functions as the structural scaffolding in the blood clotting process (*1*).

Fibrin formation on surfaces has been studied using atomic force microscopy (AFM), surface plasmon resonance (SPR) (*17*, *18*), fibrinogen-coated spheres (*19*, *20*), and a quartz crystal microbalance (*9*). Sit and Marchant used AFM to image fibrin formation on both highly ordered pyrolytic graphite (HOPG) and mica surfaces, reporting that surface

† This research was supported by the National Institutes of Health (Grant HL31048) and the National Science Foundation (Grant CHE-0349091), and a predoctoral research fellowship from the American Heart Association (K.M.E.-N.).

* To whom correspondence should be addressed. S.T.L.: e-mail, stl@med.unc.edu; phone, (919) 966-3548; fax, (919) 966-6718. M.H.S.: e-mail, schoenfi@email.unc.edu; phone, (919) 843-8714; fax, (919) 962-2388.

‡ Department of Chemistry.

§ Department of Pathology and Laboratory Medicine.

10.1021/bi0514358 CCC: $30.25
Published on Web 11/01/2005

properties influenced the polymerization process (*10*). We recently studied the influence of surface properties on fibrin proliferation from adsorbed fibrinogen using a quartz crystal microbalance (*9*). Our studies confirmed that fibrin proliferation is significantly influenced by the properties of the underlying substrate. Furthermore, the amount of fibrinogen adsorbed did not correlate to the amount of fibrin formed at each surface. Although equivalent amounts of fibrinogen adsorbed on the hydrophobic and negatively charged surfaces, little fibrin was formed at the negatively charged surface relative to the hydrophobic surface. Herein, we examine interactions of thrombin with fibrinogen on surfaces and the role of underlying substrate properties in these interactions using SPR and liquid chromatography−mass spectrometry (LC−MS). Whole fibrinogen adsorption, adsorption of individual fibrinogen domains, and thrombin-catalyzed fibrinopeptide cleavage from fibrinogen adsorbed on self-assembled monolayer surfaces presenting methyl, hydroxyl, amine, and carboxyl-terminal groups are reported.

EXPERIMENTAL PROCEDURES

Materials. Plasminogen-depleted human plasma fibrinogen (FIB1) and human α-thrombin (HT1002a) were purchased from Enzyme Research Laboratories (South Bend, IN). AaF8Y fibrinogen was provided by S.T. Lord. All protein aliquots and fibrinogen fragments were stored at −80 °C. Fibrinogen aliquots were thawed at 37 °C, stored at 5 °C when not in use, and used within 1 week of thawing. Thrombin aliquots were used the same day of thawing. Fibrinopeptide A and fibrinopeptide B standards were purchased from Sigma Scientific (St. Louis, MO). Dodecanethiol, 11-mercaptoundecanol, and 11-mercaptoundecanoic acid were also purchased from Sigma Scientific. 11-Amino-1-undecanethiol was purchased from Dojindo Scientific (Gaithersburg, MD). Undecanethiol functionalized with triethylene glycol was purchased from Prochimia (Gdansk, Poland). Thiol solutions were prepared with absolute ethanol. HEPES-buffered saline with calcium (HBSC) [0.02 M HEPES, 0.15 M NaCl, and 1 mM $CaCl_2$ (pH 7.4)] was used to prepare protein solutions and as the buffer for all experiments unless noted otherwise. Water was purified using a Milli-Q UV Gradient A10 System (Millipore Corp., Billerica, MA) to a final resistivity of 18.2 MΩ/cm and a total organic content of <6 ppb.

Preparation of the D and N-Terminal Disulfide Knot (NDSK) Fragments of Fibrinogen. To monitor the adsorption behavior of the D domain of fibrinogen, the D fragment was isolated from trypsin-cleaved fibrinogen as described previously (*21*). Briefly, fibrinogen was digested using TPCK Trypsin (Pierce, Rockford, IL) over 4 days while the extent of the reaction was monitored by SDS−PAGE. When only D fragments and E bands were visible by SDS−PAGE, the digestion was stopped. The D fragment was purified using affinity chromatography.

The adsorption of the E domain of fibrinogen was studied by isolating the central portion of the fibrinogen molecule, the N-terminal disulfide knot (NDSK). Isolation of the NDSK fragment was performed on the basis of the procedure described elsewhere (*22*). Fibrinogen was dissolved in formic acid and reacted with CNBr for 36 h under nitrogen. The CNBr was then removed by dialysis, and protein was concentrated to a final absorbance A_{280} of 60. The NDSK fragment was separated from the rest of the CNBr digestion products with an FPLC system (Amersham Biosciences, Piscataway, NJ) equipped with two sequentially connected Superdex 200 HR16/50 columns. The purified NDSK fragment ran as a single band on SDS−PAGE with an apparent molecular mass of 65 kDa and a purity of >95%.

Preparation of Gold Substrates and Self-Assembled Monolayers (SAMs). Gold substrates were prepared using glass microscope cover slips (Electron Microscopy Sciences, Washington, PA) and sterile cell culture plates (Corning Inc., Corning, NY) for surface plasmon resonance and liquid chromatography−mass spectrometry experiments, respectively. Glass microscope cover slips were cleaned by being soaked in piranha solution (3:1 H_2SO_4/H_2O_2 mixture) for at least 20 min, sonicated in milli-Q water and then ethanol, rinsed with milli-Q water, and finally dried under a stream of nitrogen. Cell culture plates were removed from sterile packaging immediately prior to being placed in the sputtering chamber and used as received. The samples were loaded into a magnetron sputtering system (Kurt Lesker Inc.), and the chamber was evacuated to 10^{-7} Torr and then backfilled with Ar to 5×10^{-3} Torr. Glass cover slips were sputtered with a 3 nm Cr adhesion layer followed by a 45 nm Au layer. Cell culture plates were directly coated with 200−300 nm Au.

Self-assembled monolayers were formed via immersion of the gold-coated cover slips or incubation of the gold-coated cell culture wells in methyl-, hydroxyl-, amino-, or carboxyl-terminated ethanolic alkanethiol solutions (∼2 mM) overnight. The hydrophobicity and the charge of the surfaces resulting from the described preparation method were verified through previous work (*9*). Alkanethiol self-assembled monolayers have been used extensively as model surfaces for a range of surface studies, including protein adsorption and cell adhesion (*23*).

Surface Plasmon Resonance (SPR). Surface plasmon resonance experiments were performed using a BIAcore X instrument (Biacore, Inc., Uppsala, Sweden). A continuous flow of buffer was maintained throughout the experiments, with the analyte of interest injected for controlled periods of time. Adsorption of D and E domains was carried out at a flow rate of 10 μL/min in HEPES-buffered saline without calcium (HBS) [0.02 M HEPES and 0.15 M NaCl (pH 7.4)]. After a stable baseline had been established, a 0.3 μM solution of either D or E domain was injected for 10 min and then the mixture rinsed with buffer for 10 min. Fibrinogen adsorption and thrombin cleavage experiments were completed using a constant HBSC buffer flow rate of 4 μL/min. HEPES-buffered saline with calcium was used for all fibrinogen adsorption and cleavage experiments to ensure a consistent calcium concentration and avoid discrepancies from experiment to experiment due to variations in inevitable trace (contaminant) calcium content. The lower flow rate was used to allow thrombin to flow over adsorbed fibrinogen for a longer period, given the limited injection loop volume of 100 μL. Fibrinogen (1 mg/mL) was injected into the flow cell for 10 min, and the flow cell was rinsed with HBSC buffer for 10 min. Thrombin (1 unit/mL) was then injected into the flow cell for 25 min, and the cell was again rinsed with HBSC for 10 min. In separate experiments, varying the flow rate and calcium concentration had little

effect on the amounts of fibrinogen adsorbed on each surface (data not shown).

Cleavage of Fibrinopeptides from Adsorbed Fibrinogen. Fibrinogen was adsorbed on SAM-modified gold-coated wells in cell culture plates after incubation of the wells with 2.5 mL of a 1 mg/mL fibrinogen solution for 10 min. The fibrinogen solution was then poured from the wells and subjected to three rinsing steps. (1) The plate was immersed in a ~750 mL buffer reservoir under gentle shaking conditions for 3 min. (2) Rinsing step 1 was repeated. (3) The wells were rigorously rinsed with buffer individually for 6 min. This total rinsing time of 10 min is analogous to the 10 min rinsing period used in SPR experiments after injection of fibrinogen. After the wells had been rinsed, a thrombin solution (1 unit/mL, 9 nM) was added. Aliquots of 110 μL were removed at time intervals of 0.5, 1, 3, 7, 15, 30, 60, and either 90 or 105 min. To verify nonadsorbed protein was completely removed during the rinsing procedure, control experiments were conducted in wells modified with polyethylene glycol-terminated SAMs, which adsorb negligible amounts of fibrinogen (as verified with SPR). Fibrinopeptides were not observed in aliquots analyzed from these control wells.

A 100 μL sample from each aliquot was injected into an Agilent 1100 series liquid chromatography system with a mass spectrometer (Agilent MSD-SL) as a detector. Fibrinopeptides A and B were separated and desalted on a Hypersil ODS C18 column (4.6 mm × 100 mm, 3 μm). The solvent system was 0.05% trifluoroacetic acid in water (solvent A) and 0.05% trifluoroacetic acid in acetonitrile (solvent B). The system was initially equilibrated in 100% solvent A and 0% solvent B for 1 min, and then the mixture was changed to 15% solvent B in a linear gradient during the next minute and then changed in a linear gradient to 36% solvent B between minutes 2 and 25. After each run, the system was flushed for 5 min in 80% solvent B and then changed to 100% solvent A for 4 min. The electrospray ionization capillary was held at 3000 V with a drying gas flow rate of 12 L/min and a drying gas temperature of 350 °C. The mass spectrometer was set to selectively monitor the +2 ions of fibrinopeptide A at *m*/*z* 769 and fibrinopeptide B at *m*/*z* 777. Calibration curves were generated for each batch of samples using 100 μL of mixed fibrinopeptide A and fibrinopeptide B standard solutions at concentrations of 1.5, 3, 6, 12, and 24 nM. The concentrations of fibrinopeptides A and B in aliquots removed from the cell culture plate wells at specific time intervals were calculated on the basis of the calibration curve. The total number of picomoles per square centimeter released was then calculated on the basis of the volume of solution in the wells and the surface area of the wells exposed to solution. The reduction in volume due to removal of 110 μL for each aliquot was included in these calculations.

RESULTS

Adsorption of Fibrinogen and Fibrinogen Fragments. We monitored the adsorption of fibrinogen to SAMs presenting methyl-, hydroxyl-, amine-, and carboxyl-terminal groups using SPR. Representative SPR sensorgrams of whole fibrinogen adsorption at each surface studied are shown in Figure 1. The SPR response signal for fibrinogen adsorption at the methyl surface was consistent with a prior SPR report using similar experimental methods and instrumentation (*5*). As shown in Figure 1, after the flow cell had been flushed with HBSC to allow desorption of reversibly adsorbed fibrinogen ($t = 22$ min), the amount of fibrinogen irreversibly adsorbed on methyl-, amine-, and carboxyl-terminated SAMs was comparable. Significantly less fibrinogen adsorbed to hydroxyl SAMs. These trends were consistent with previous studies (*9*, *24*).

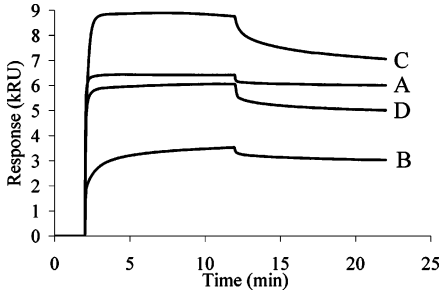

FIGURE 1: Representative surface plasmon resonance sensorgrams for fibrinogen adsorption at (A) methyl-, (B) hydroxyl-, (C) amine-, and (D) carboxyl-terminated self-assembled monolayers. Fibrinogen was injected at 2 min to initiate protein adsorption. Kilo-response units (kRU) are proportional to surface mass.

The rapid decrease in signal of ~0.2 kRU occurring immediately after fibrinogen was rinsed from the cell (Figure 1, $t = 12$ min) does not represent desorption of fibrinogen, but is rather attributed to differences in the bulk refractive index of a fibrinogen solution and HBSC. The signal decrease occurring at each surface after the initial refractive index decrease is due to protein desorption. Although fibrinogen adsorption on surfaces is largely irreversible (*25*), some desorption was observed as indicated by the continued decrease in sensorgram response for certain surfaces (Figure 1, curves B, C and D). Hydrophobic effects are largely responsible for irreversible protein adsorption, while weaker electrostatic attractions lead to more reversible interactions (*26*). Therefore, the rapid adsorption of fibrinogen at the methyl surface was largely irreversible (Figure 1, curve A), whereas slower adsorption and more extensive desorption kinetics were observed at the hydroxyl surfaces where hydrophobic effects do not influence surface−protein interactions as significantly (Figure 1, curve B). At the charged surfaces, more desorption (Figure 1, curves C and D) occurred because a greater population of the fibrinogen was most likely held to the surface through electrostatic interactions. Although fibrinogen is a large protein with regions of both positive and negative charge, the overall charge of the protein is negative (*13*). As such, the largest amount of fibrinogen adsorption was observed at the amine-terminated SAM. However, this surface was characterized also by the greatest overall protein desorption upon rinsing of the flow cell (Figure 1, curve C).

The adsorption of the D and NDSK fragments of fibrinogen, termed hereafter the D and E domains, respectively, was also examined. Of note, fibrinogen molecules are larger and cover more surface area than either the D or E domain. As expected due to size, larger amounts of both the D and E domains adsorbed on each surface than did whole fibrinogen (Table 1). Like the fibrinogen adsorption trends, comparable amounts of E domain adsorbed on the methyl-, amine-, and carboxyl-terminated alkanethiol SAMs, while a reduced amount of E domain adsorbed on the hydroxyl-

Table 1: Adsorption of Whole Fibrinogen, the D Domain, and the E Domain

surface terminal group	pmol of fibrinogen adsorbed/cm^2	pmol of D domain adsorbed/cm^2	pmol of NDSK domain adsorbed/cm^2	D/fgn ratio	E/fgn ratio
methyl	1.7 ± 0.2	3.4 ± 0.1	2.9 ± 0.2	2.0 ± 0.2	1.7 ± 0.2
hydroxyl	0.85 ± 0.06	2.1 ± 0.2	1.4 ± 0.1	2.5 ± 0.3	1.6 ± 0.2
amine	1.9 ± 0.2	2.8 ± 0.1	3.3 ± 0.2	1.4 ± 0.2	1.7 ± 0.2
carboxyl	1.4 ± 0.1	4.2 ± 0.4	2.9 ± 0.3	3.0 ± 0.4	2.1 ± 0.3

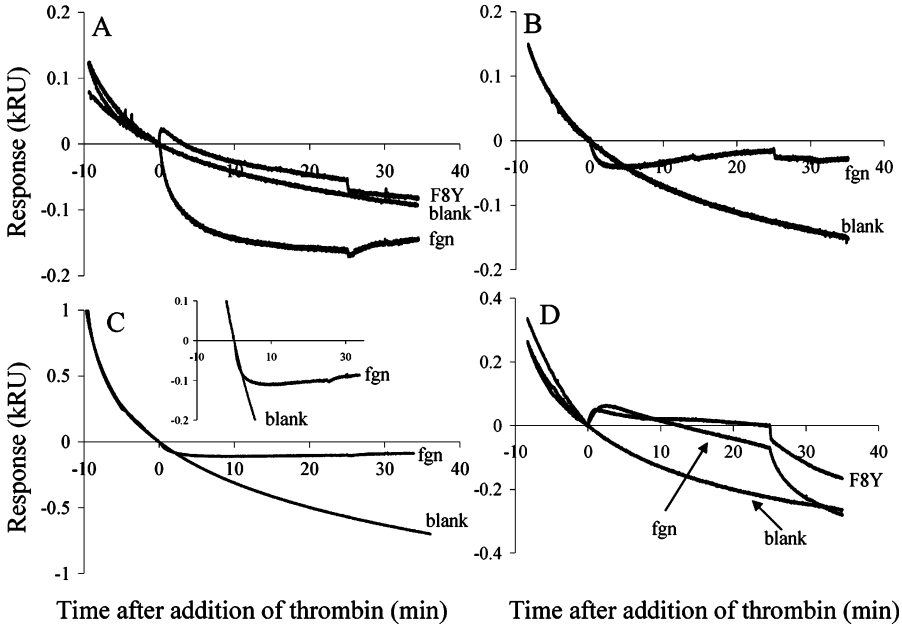

FIGURE 2: Surface plasmon resonance sensorgrams upon addition of thrombin to plasma fibrinogen (fgn) and AαF8Y fibrinogen (F8Y) adsorbed at (A) methyl-, (B) hydroxyl-, (C) amine-, and (D) carboxyl-terminated self-assembled monolayers and SPR signal during control experiments where no thrombin was added (blank). The response and time axes are zeroed to 20 min after the initial injection of fibrinogen, the time when thrombin was injected in the noncontrol experiments. The inset represents the sensorgram for panel C on a scale comparable to that shown for the other surfaces.

modified surfaces. Although the absolute amount of E domain adsorbed was greater than the amount of fibrinogen adsorbed on each surface, the amount of E domain adsorbed relative to the amount of fibrinogen adsorbed was constant between surfaces (Table 1, E/fgn ratio).

Consistent with the E domain, larger amounts of D domain than of whole fibrinogen adsorbed to the surfaces. In contrast to the E domain, the trends for D domain adsorption were not consistent with the adsorption trends for whole fibrinogen. This distinction is reflected in the differing D domain/fibrinogen ratios between the surfaces (Table 1, D/fgn ratio). Rather than being constant, the ratios for the surfaces varied as follows: carboxyl-terminated = hydroxyl-terminated > methyl-terminated > amine-terminated alkanethiol self-assembled monolayers. These data demonstrate that the dependencies of whole fibrinogen and E domain adsorption on surface properties are equivalent, but different from that for the D domain.

Exposure of Adsorbed Fibrinogen to Thrombin. The conversion of adsorbed fibrinogen to fibrin monomer was examined using SPR by passing thrombin over preadsorbed fibrinogen. Representative SPR sensorgrams are shown in Figure 2. The signal was re-zeroed 20 min after fibrinogen injection (t = 22 min in Figure 1, t = 0 min in Figure 2), when either thrombin was injected or buffer flow was continued; the signals from the latter are labeled as the control in Figure 2. When fibrinogen (fgn) adsorbed on the methyl (Figure 2A), hydroxyl (Figure 2B), and amine (Figure 2C) surfaces was exposed to thrombin, a rapid decrease in the magnitude of the signal was observed, resulting in a mass loss of 2.0 ± 0.3% from the methyl SAM and 1.2 ± 0.1% from the amine SAM. As the mass of fibrinopeptides cleaved from fibrinogen ($2 \times \text{mass}_{\text{FpA}} + 2 \times \text{mass}_{\text{FpB}}$) is 1.8% of the total mass of the molecule (calculated using the amino acid composition of FpA and FpB, and the molecular mass of fibrinogen), the measured decrease in mass at the methyl- and amine-terminated SAMs correlated well with that expected for fibrinopeptide cleavage. The mass decrease from the hydroxyl-terminated SAM was much smaller (0.2 ± 0.7%).

The decreasing mass prior to the injection of thrombin at time zero (Figure 1) is attributed to desorption of reversibly bound fibrinogen molecules (*25*). Although this desorption is minor relative to the overall adsorption of fibrinogen, the signal is significant on the scale of thrombin-catalyzed fibrinopeptide cleavage (Figure 2). In control experiments, a continual decrease in the magnitude of the signal throughout the experiment corresponding to protein desorption was noted (Figure 2, blank). However, fibrinogen desorption at the methyl-, hydroxyl-, and amine-terminated SAMs ceased after exposure to thrombin, indicating the conversion of adsorbed fibrinogen to fibrin enhances the stability of the adsorbed layer. In contrast, an increase in signal was noted on the carboxyl-modified SAM immediately after addition of thrombin to fibrinogen, which was followed by desorption after thrombin was flushed from the flow cell. The initial

increase in the magnitude of the signal suggests thrombin association with the adsorbed fibrinogen, nonspecific thrombin association with the negatively charged underlying substrate (to which fibrinogen is adsorbed), or both.

To further explore the role of thrombin in the observed change in mass, we evaluated interaction of thrombin with an adsorbed recombinant fibrinogen, AαF8Y, where a phenylalanine has been changed to a tyrosine on the Aα chain. Since phenylalanine (F in the single-letter annotation) at position 8 of the Aα chain is critical for FpA cleavage, AαF8Y fibrinogen represents a poor thrombin substrate even though thrombin binding is normal (*27*). Therefore, we anticipated that exposing adsorbed AαF8Y fibrinogen to thrombin would only show decreases in mass corresponding to continued fibrinogen desorption. We conducted these experiments using the methyl- and carboxyl-modified surfaces. As shown in Figure 2A, F8Y, a rapid decrease in the magnitude of the signal associated with fibrinopeptide cleavage was not observed with AαF8Y fibrinogen adsorbed on the methyl-terminated SAM. Indeed, desorption continued both during and after the injection of thrombin.

At the carboxyl-terminated SAM, we noted an obvious association of thrombin with both adsorbed plasma fibrinogen and AαF8Y fibrinogen as evidenced by an increase in the strength of the sensorgram response (Figure 2D). After the initial increase in the magnitude of the signal, the sensorgram response decreased for both surfaces, consistent with continued desorption. The rate of protein desorption for normal fibrinogen was greater than that for the variant, indicating both desorption and limited cleavage were taking place with the plasma fibrinogen. After thrombin was rinsed from the flow cell, comparable rates of the decrease in the magnitude of the signal were observed (thrombin dissociation and continued fibrinogen desorption). Since desorption continues after exposure of either adsorbed AαF8Y or plasma fibrinogen to thrombin at the carboxyl-modified SAM, we conclude that neither protein was substantially converted to fibrin. In contrast, cleavage of fibrinopeptides from plasma fibrinogen was obvious at the methyl-, hydroxyl-, and amine-terminated SAMs, and subsequent desorption from these surfaces was minimal, indicating most of the fibrinogen was converted to fibrin.

We also confirmed differences between the signals following exposure of thrombin to adsorbed plasma fibrinogen and adsorbed AαF8Y fibrinogen were not related to protein structure. Indeed, fibrinopeptide cleavage for normal recombinant fibrinogen at a methyl-terminated SAM was comparable to fibrinopeptide cleavage from plasma fibrinogen. Desorption of recombinant fibrinogen also ceased after thrombin exposure (data not shown), as in the plasma fibrinogen experiments.

LC−MS Analysis of Release of Fibrinopeptides from Adsorbed Fibrinogen. Release of fibrinopeptides from adsorbed fibrinogen was assessed to confirm the surface dependence observed in the SPR data. To obtain sufficient peptide to quantify such release, we performed these studies using fibrinogen adsorbed in culture dishes as described in Experimental Procedures. Release of fibrinopeptides from adsorbed fibrinogen was assessed as a function of time after the addition of thrombin, as shown in Figure 3. The percentage of FpA and FpB released from fibrinogen adsorbed on each SAM (Table 1, % FpA cleaved and

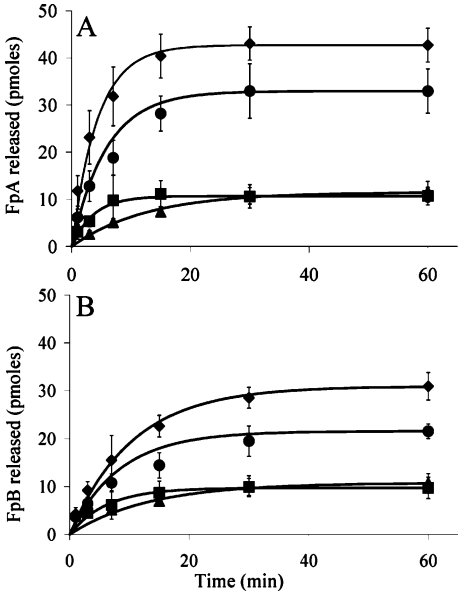

FIGURE 3: Release of fibrinopeptide A (A) and fibrinopeptide B (B) from fibrinogen adsorbed at (●) methyl-, (■) hydroxyl-, (◆) amine-, and (▲) carboxyl-terminated self-assembled monolayers ($n = 5$ for each surface) as measured by LC−MS. The curves are based on fits of normalized data assuming first-order rate kinetics.

Table 2: Comparison of Fibrinopeptide Cleavage with the Amount of Fibrinogen Adsorbed

surface terminal group	pmol of FpA cleaved/cm^2	pmol of FpB cleaved/cm^2	% FpA cleaved	% FpB cleaved
methyl	2.7 ± 0.4	1.8 ± 0.2	78 ± 13	52 ± 7
hydroxyl	0.9 ± 0.2	0.8 ± 0.1	51 ± 9	46 ± 8
amine	3.5 ± 0.3	2.5 ± 0.2	91 ± 13	65 ± 9
carboxyl	0.9 ± 0.2	0.9 ± 0.2	33 ± 7	30 ± 7

% FpB cleaved) was calculated using the fibrinogen surface coverage obtained with SPR (Table 1, picomoles of fgn adsorbed per square centimeter) and the total FpA and FpB released at 60 s (Table 1, picomoles of FpA cleaved per square centimeter and picomoles of FpB cleaved per square centimeter). The amount of fibrinogen adsorbed on the surface was calculated using the published BIAcore response unit conversion factor (*28*) and a fibrinogen molecular weight of 340 000 (*15*). The amount of fibrinogen adsorbed on the methyl SAM substrate correlated well with previously published values (*24*, *29*, *30*). The amount (picomoles per square centimeter) of fibrinopeptides released from the wells of the cell culture plates was calculated on the basis of the known number of picomoles of fibrinopeptide released and the surface area of a well filled with 2.5 mL of solution. The % FpA and % FpB cleavage values reported in Table 1 were calculated considering that each mole of fibrinogen adsorbed has 2 mol of FpA and 2 mol of FpB.

As shown in Table 3, the rate of release of FpA from fibrinogen adsorbed on the carboxyl-terminated SAM was significantly slower than that from fibrinogen adsorbed on the methyl-, hydroxyl-, and amine-terminated alkanethiol SAMs. In contrast, fibrinopeptide B release was comparable for each SAM. The kinetics of release of FpB from adsorbed fibrinogen did not fit the model typically used for release of FpB from fibrinogen in solution (*31*). In solution, fibrinopeptide release follows sequential first-order kinetics with FpA preceding FpB release (*15*, *16*). In other words, FpB release is delayed in solution. Release of fibrinopeptides from

Table 3: First-Order Rate Constants (min^{-1}) for Fibrinopeptide Cleavage

surface terminal group	fibrinopeptide A	fibrinopeptide B
methyl	0.17 ± 0.05	0.13 ± 0.06
hydroxyl	0.22 ± 0.04	0.16 ± 0.04
amine	0.25 ± 0.09	0.10 ± 0.02
carboxyl	0.071 ± 0.003	0.09 ± 0.03

adsorbed fibrinogen also follows first-order kinetics, but cleavage of FpB from adsorbed fibrinogen does not depend on the prior release of FpA. Fibrinopeptides A and B were released simultaneously from fibrinogen adsorbed on each SAM surface. As shown in Table 3, the rates of FpA and FpB release were similar at each surface, except at the amine-terminated SAM, where FpA release occurred more rapidly than FpB release.

DISCUSSION

Herein, we have systematically studied the interactions of thrombin with fibrinogen adsorbed on model surfaces. Interactions of thrombin with fibrinogen adsorbed on each SAM surface differed significantly from the interactions of thrombin with fibrinogen in solution. The behavior or activity of adsorbed fibrinogen is known to differ from that of solution fibrinogen. For example, platelets do not adhere to fibrinogen dissolved in solution, but will adhere to fibrinogen adsorbed on a surface (*6*). Furthermore, the adsorption of fibrinogen has been reported to induce conformational changes in the D domain, revealing epitopes that facilitate phagocyte binding (*32*). On the basis of our data, the adsorption of fibrinogen to a surface also alters subsequent fibrinogen−thrombin interactions. Specifically, the sequence and rate of fibrinopeptide release were different for solution and adsorbed fibrinogen. In solution, FpA release precedes FpB release (*14*). Mullin and co-workers have hypothesized that a conformational change known to accompany FpA cleavage (*33*) may facilitate FpB cleavage, thus explaining the lag in FpB cleavage in solution (*34*). We did not observe a lag in FpB cleavage, but rather concurrent release of FpA and FpB from surface-adsorbed fibrinogen upon thrombin exposure. In fact, concurrent release of FpA and FpB was observed from fibrinogen adsorbed on each model substrate, regardless of the underlying substrate properties. Jirouskova et al. observed similar cleavage of fibrinopeptides from fibrinogen adsorbed to glass surfaces (*35*).

As previously reported, release of both FpA and FpB from AαF8Y fibrinogen is impaired, even though only the Aα chain is modified (*27*). It was assumed that FpB cleavage was negligible because FpA was not cleaved and FpB release follows FpA release. On the basis of the independent release of FpA and FpB from adsorbed fibrinogen observed herein, it could be assumed that release of FpB would proceed normally from adsorbed AαF8Y fibrinogen. However, release of FpB from adsorbed AαF8Y fibrinogen was not observed in the SPR sensorgrams (Figure 2D). As the mass loss due to FpB release is smaller and likely slower than that for FpA, the release of FpB may be indiscernible from AαF8Y fibrinogen desorption using SPR.

The rates of release of fibrinopeptides from adsorbed fibrinogen also differed from those observed in solution. In a previous report, >90% of FpA was released ~3 min after addition of thrombin (9 nM) to fibrinogen (22 μM) in experiments [fibrinogen/thrombin ratio of 2400/1 (*36*)]. However, release of FpA the hydroxyl- and amine-terminated SAMs (the two surfaces with the fastest fibrinopeptide cleavage rates) reached 90% ~9 min after the addition of thrombin. Additionally, the ratio of fibrinogen to thrombin was several orders of magnitude lower for the LC−MS fibrinopeptide cleavage experiments described herein (~1:1). Higher concentrations of thrombin were employed to avoid mass transport effects and to observe the maximum possible rate of cleavage of fibrinopeptide from adsorbed fibrinogen. Regardless of the properties of the underlying substrate, the adsorption of fibrinogen slowed FpA release considerably relative to previously reported rates for fibrinogen in solution.

Interactions of thrombin with adsorbed fibrinogen also varied with the surface. The effect of surface properties on thrombin-adsorbed fibrinogen interactions paralleled the previously reported influence of surface properties on fibrin proliferation at model surfaces (*9*). Indeed, the amount of FpA and FpB released, the rate of FpA release, and the SPR signal for exposure of thrombin to fibrinogen indicate that thrombin activity with adsorbed fibrinogen was most efficient at methyl- and amine-terminated SAMs, less efficient at the hydroxyl-terminated SAM, and inefficient at the carboxyl-terminated SAM. The correlation between the influence of surface properties on fibrin proliferation and on adsorbed fibrinogen−thrombin interactions indicates that these interactions dictate the extent of fibrin proliferation on a surface.

Both the electrostatic environment of the surfaces and the conformational changes in fibrinogen upon adsorption could significantly influence adsorbed fibrinogen−thrombin interactions. Fenton and co-workers found thrombin was nonspecifically attracted to a negatively charged surface even though thrombin is a predominantly uncharged protein (*37*). On the basis of studies of the zymogen precursor prothrombin and thrombin inhibited by the peptide hirudin, they inferred thrombin binds nonspecifically to negatively charged surfaces via cationic clusters critical in binding the enzyme to fibrinogen in the correct orientation for catalysis of fibrinopeptide cleavage. We observed a mass increase for both plasma and AαF8Y fibrinogens consistent with nonspecific attraction of thrombin to fibrinogen adsorbed on the carboxyl-terminated SAM (Figure 2). Additionally, we found fibrinogen adsorbed on the carboxyl-terminated SAM was ineffective at catalyzing fibrinopeptide cleavage, relative to fibrinogen adsorbed on the other surfaces. It is feasible that thrombin was nonspecifically attracted to the fibrinogen adsorbed on the carboxyl-terminated SAM, because of the underlying charge, in a manner that disrupted proper binding to fibrinogen and/or catalysis of fibrinopeptide cleavage.

The conformation of adsorbed fibrinogen could also influence thrombin−fibrinogen interactions. The extent and nature of conformational changes occurring upon adsorption depend on the underlying surface. Sit and Marchant observed surface-dependent conformational changes in fibrinogen adsorbed on hydrophobic, negatively charged, and positively charged substrates using atomic force microscopy (*38*). They reported significantly greater spreading of fibrinogen adsorbed on the hydrophobic and positively charged surfaces than on negatively charged surfaces. In this study, we

observed differences in the extent of binding of the D and E domains depending on the charge and hydrophobicity of the underlying surface. As shown in Table 2 (D/fgn ratio), the ratio of the amount of D domain adsorbed relative to whole fibrinogen was significantly lower at the methyl- and amine-terminated SAMs than at the hydroxyl- and carboxyl-terminated SAMs while the amount of E domain adsorbed relative to whole fibrinogen was equivalent at all surfaces (Table 2, E/fgn ratio). These data suggest the D domain was prone to extensive spreading at the methyl- and amine-terminated SAMs, while the E domain did not spread significantly at any surface. The D domain has a net negative charge (*13*) and is known to be more labile than the E domain, unfolding more easily. Spreading of the D domain at the methyl- and amine-terminated SAMs correlates with the extent of fibrinopeptide cleavage observed with SPR and LC−MS, indicating that spreading may be significant in adsorbed fibrinogen interactions.

In summary, we have studied interactions of thrombin with fibrinogen adsorbed on model substrates with varying surface charge and hydrophobicity. Thrombin-catalyzed fibrinopeptide cleavage of fibrinogen adsorbed at each surface was impaired, relative to that of fibrinogen in solution. We found the amount of fibrinopeptide cleavage, the rate of FpA cleavage, the extent of conversion of adsorbed fibrinogen to fibrin, and conformational changes in the D domain of fibrinogen were all diminished at carboxyl-terminated SAM. The dependence of adsorbed fibrinogen−thrombin interactions on surface charge and wettability directly reflected previously reported trends regarding the dependence of fibrin proliferation on surfaces on the properties of the underlying substrate. Notably, fibrin proliferation at negatively charged surfaces was significantly less efficient than at hydrophobic-, hydroxyl-, and amine-modified surfaces (*9*). We conclude that the interactions of thrombin with surface-adsorbed fibrinogen dictate subsequent fibrin proliferation. Ongoing work is focused on elucidating the structural changes in the adsorbed protein layer when adsorbed fibrinogen is converted to fibrin, and using LC−MS to quantify the release of FpB from adsorbed AαF8Y fibrinogen.

ACKNOWLEDGMENT

We thank Li Fang Ping for assistance in preparing and characterizing fibrinogen fragments (D and NDSK) and AαF8Y recombinant fibrinogen. We also thank David Black for assistance with LC−MS analysis.

REFERENCES

1. Avramoglou, T., Jozefonvicz, J., and Jozefowicz, M. (2002) Blood-contacting polymers, *Polym. Biomater. (2nd Ed.)*, 611−646.
2. Horbett, T. A. (1999) The role of adsorbed adhesion proteins in cellular recognition of biomaterials, *BMES Bull. 23*, 5−9.
3. Ratner, B. D., and Bryant, S. J. (2004) Biomaterials: Where we have been and where we are going, *Annu. Rev. Biomed. Eng. 6*, 41−75.
4. Anderson, J. M. (2001) Biological responses to materials, *Annu. Rev. Mater. Res. 31*, 81−110.
5. Ostuni, E., Chapman, R. G., Holmlin, E. R., Takayama, S., and Whitesides, G. M. (2001) A survey of structure−property relationships of surfaces that resist the adsorption of protein, *Langmuir 17*, 5605−5620.
6. Tsai, W.-B., Grunkemeier, J. M., and Horbett, T. A. (1999) Human plasma fibrinogen adsorption and platelet adhesion to polystyrene, *J. Biomed. Mater. Res. 44*, 130−139.
7. Tsai, W.-B., Grunkemeier, J. M., and Horbett, T. A. (2003) Variations in the ability of adsorbed fibrinogen to mediate platelet adhesion to polystyrene-based materials: A multivariate statistical analysis of antibody binding to the platelet binding sites of fibrinogen, *J. Biomed. Mater. Res. 67A*, 1255−1268.
8. Tsai, W.-B., Grunkemeier, J. M., McFarland, C. D., and Horbett, T. A. (2002) Platelet adhesion to polystyrene-based surfaces preadsorbed with plasmas selectively depleted in fibrinogen, vitronectin, or Von Willebrand's factor, *J. Biomed. Mater. Res. 60*, 348−359.
9. Evans-Nguyen, K. M., and Schoenfisch, M. H. (2005) Fibrin proliferation at model surfaces: influence of surface properties, *Langmuir 21*, 1691−1694.
10. Sit, S. P., and Marchant, R. E. (2001) Surface-dependent differences in fibrin assembly visualized by atomic force microscopy, *Surf. Sci. 491*, 421−432.
11. Andrade, J. D. (1985) Principles of Protein Adsorption, in *Surface and interfacial aspects of biomedical polymers* (Andrade, J. D., Ed.) Plenum Press, New York.
12. Andrade, J. D., and Hlady, V. (1987) Plasma Protein Adsorption: The Big Twelve, in *Blood in Contact with Natural and Artificial Surfaces* (Leonard, E. F., Turitto, V. T., and Vroman, L., Eds.) pp 158−172, New York Academy of Sciences, New York.
13. Feng, L., and Andrade, J. D. (1995) Structure and Adsorption Properties of Fibrinogen, in *Proteins at Interfaces II: Fundamentals and Applications* (Horbett, T. A., and Brash, J. L., Eds.) American Chemical Society, Washington, DC.
14. Weisel, J. W. (2005) Fibrinogen and fibrin, *Adv. Protein Chem. 70*, 247−299.
15. Blomback, B. (1996) Fibrinogen and fibrin: proteins with complex roles in hemostasis and thrombosis, *Thromb. Res. 83*, 1−75.
16. Binnie, C. G., and Lord, S. T. (1993) The fibrinogen sequences that interact with thrombin, *Blood 81*, 3186−3192.
17. Dyr, J. E., Rysava, J., Suttnar, J., Homola, J., and Tobiska, P. (2001) Optical sensing of the initial stages in the growth and development of fibrin clot, *Sens. Actuators, B 74*, 69−73.
18. Rysava, J., Dyr, J. E., Homola, J., Dostalek, J., Krizova, P., Masova, L., Suttnar, J., Briestensky, J., Santar, I., Myska, K., and Pecka, M. (2003) Surface interactions of oxidized cellulose with fibrin(ogen) and blood platelets, *Sens. Actuators, B 90*, 243−249.
19. Retzinger, G. S., DeAnglis, A. P., and Patuto, S. J. (1998) Adsorption of fibrinogen to droplets of liquid hydrophobic phases: Functionality of the bound protein and biological implications, *Arterioscler. Thromb. Vasc. Biol. 18*, 1948−1957.
20. Whitlock, P. W., Clarson, S. J., and Retzinger, G. S. (1999) Fibrinogen adsorbs from aqueous media to microscopic droplets of poly(dimethoxysiloxane) and remains coagulable, *J. Biomed. Mater. Res. 45*, 55−61.
21. Kostelansky, M. S., Betts, L., Gorkun, O. V., and Lord, S. T. (2002) 2.8 Å crystal structures of recombinant fibrinogen fragment d with and without two peptide ligands: GHRP binding to the "b" site disrupts its nearby calcium-binding site, *Biochemistry 41*, 12124−12132.
22. Blomback, B., Hessel, B., Iwanaga, S., Reuterby, J., and Blomback, M. (1972) Primary structure of human fibrinogen and fibrin. I. Clevage of fibrinogen with cyanogen bromide. Isolation and characterization of NH_2-terminal fragments of the ("A") chain, *J. Biol. Chem. 247*, 1496−512.
23. Ostuni, E. Y. L., and Whitesides, G. M. (1999) The interaction of proteins and cells with self-assembled monolayers of alkanethiolates on gold and silver, *Colloids Surf., B 15*, 3−30.
24. Sigal, G. B., Mrksich, M., and Whitesides, G. M. (1998) Effect of surface wettability on the adsorption of proteins and detergents, *J. Am. Chem. Soc. 120*, 3463−3473.
25. Wertz, C. F., and Santore, M. M. (2002) Fibrinogen adsorption on hydrophilic and hydrophobic surfaces: geometrical and energetic aspects of interfacial relaxations, *Langmuir 18*, 706−715.
26. Norde, W. (2003) Driving forces for protein adsorption at solid surfaces, *Surfactant Sci. Ser. 110*, 21−43.
27. Rooney, M. M., Mullin, J. L., and Lord, S. T. (1998) Substitution of tyrosine for phenylalanine in fibrinopeptide A results in preferential thrombin cleavage of fibrinopeptide B from fibrinogen, *Biochemistry 37*, 13704−13709.
28. Karlsson, R., Roos, H., Faegerstam, L., and Persson, B. (1994) Kinetic and concentration analysis using BIA technology, *Methods 6*, 99−110.

29. Werner, C., Eichhorn, K. J., Grundke, K., Simon, F., Grahlert, W., and Jacobasch, H. J. (1999) Insights on structural variations of protein adsorption layers on hydrophobic fluorohydrocarbon polymers gained by spectroscopic ellipsometry. Part I, *Colloids Surf., A 156*, 3−17.
30. Wojciechowski, P. W., and Brash, J. L. (1993) Fibrinogen and albumin adsorption from human blood onto chemically functionalized silica substrates, *Colloids Surf., B 1*, 107−117.
31. Ng, A. S., Lewis, S. D., and Shafer, J. A. (1993) Quantifying thrombin-catalyzed release of fibrinopeptides from fibrinogen using high-performance liquid chromatography, *Methods Enzymol. 222*, 341−58.
32. Hu, W.-J., Eaton, J. W., and Tang, L. (2001) Molecular basis of biomaterial-mediated foreign body reactions, *Blood 98*, 1231−1238.
33. Henschen-Edman, A. H. (1997) Photo-oxidation of histidine as a probe for aminoterminal conformational changes during fibrinogen-fibrin conversion, *Cell. Mol. Life Sci. 53*, 29−33.
34. Mullin, J. L., Gorkun, O. V., Binnie, C. G., and Lord, S. T. (2000) Recombinant fibrinogen studies reveal that thrombin specificity dictates order of fibrinopeptide release, *J. Biol. Chem. 275*, 25239−25246.
35. Jirouskova, M., Dyr, J. E., Suttnar, J., Holada, K., and Trnkova, B. (1997) Platelet adhesion to fibrinogen, fibrin monomer, and fibrin protofibrils in flowing blood. The effect of fibrinogen immobilization and fibrin formation, *Thromb. Haemostasis 78*, 1125−1131.
36. Mihalyi, E. (1988) Clotting of bovine fibrinogen. Kinetic analysis of the release of fibrinopeptides by thrombin and of the calcium uptake upon clotting at high fibrinogen concentrations, *Biochemistry 27*, 976−82.
37. Fenton, J. W., Olson, T. A., Zabinsky, M. P., and Wilner, G. D. (1988) Anion-binding exosite of human α-thrombin and fibrin(ogen) recognition, *Biochemistry 27*, 7106−7112.
38. Sit, P. S., and Marchant, R. E. (1999) Surface-dependent conformations of human fibrinogen observed by atomic force microscopy under aqueous conditions, *Thromb. Haemostasis 82*, 1053−1060.

BI0514358